

Photocatalysis

Nanoflower-Like Bi₂WO₆ Encapsulated in ORMOSIL as a Novel Photocatalytic Antifouling and Foul-Release CoatingGabriele Scandura,^[a] Rosaria Ciriminna,^[b] Yi-Jun Xu,^[c] Mario Pagliaro,^{*[b]} and Giovanni Palmisano^{*[a]}

Abstract: Herein, the first multi-purpose antifouling and foul-release photocatalytic coating based on ORMOSIL thin films doped with nanoflower-like Bi₂WO₆ is described. Irradiation with visible light of the new films immersed in water produces significant amounts of H₂O₂ by photocatalytic oxidation of water, and allows the degradation of (bio)organic pollutants at the outer surface of the xerogel film.

Marine biofouling is an important global economic problem costing several US billion \$ per year in transportation costs due to increased fuel consumption from added drag.^[1] Bacteria naturally present in seawater (and in fluvial environments) as well as diatoms, algae, and invertebrates form a biofilm on any immersed surface within 48 h. Furthermore, these biofilms often lead to microbially induced corrosion (MIC) due to H₂S created by specific types of bacteria. If the hull's surface roughens then hydrodynamic drag increases leading either to enhanced fuel consumption or to reduced speed. After some months, a ship without antifouling (AF) paint will use more fuel due to additional hull drag from fouling.^[2] To immediately grasp the relevance of antifouling coatings, it is enough to consider that if no antifouling paint was coated on the 39,000 vessels comprising the world's fleet in 1994, an extra 72 million tonnes of bunker fuel would have been burned besides the 184 million tonnes actually consumed. That year, the whole North Sea oil production equated to 100 million tonnes.^[3]

Every year, more than 80,000 tonnes of marine AF paints, mostly copper-based, are used across the world,^[4] replacing

highly toxic tributyl-tin widely used in AF formulations until 2008 when the 1999 International Maritime Organization (IMO) International Convention on the Control of Harmful Antifouling Systems on Ships came into force. Intense research carried out at both antifouling coatings makers and in the academy has resulted in the development of several environmentally benign alternatives,^[5] mostly based on foul-release (FR) marine coatings, but including also formulations, the action of which is based on less toxic biocides, and even on the photocatalytic activity of dye-sensitized ZnO nanoparticles.^[6] In this context, sol-gel derived functional coatings based on amorphous silicas are suitable alternative FR marine coatings.^[7] Organosilica-based coatings, indeed, cure at room temperature, are economically and environmentally friendly, and easily bind to all type of surfaces (steel, fiberglass, aluminum, and wood) by a variety of means including spraying, brushing or rolling, dip-coating and spin-coating. Moreover, xerogel films prepared by the sol-gel process are porous and permeable towards different ions and neutral molecules, and the hydrophilic-lipophilic balance (HLB) can be controlled by the precursors and the processing conditions.^[8]

Another important aspect is that functional species can be sequestered within the xerogel retaining, and often enhancing, the chemical reactivity observed in solution.^[8,9] Bright, Detty, and co-workers in 2009 first reported that organically modified silicate (ORMOSIL) coatings derived from the sol-gel polycondensation of aminopropyltriethoxysilane and tetraethyl orthosilicate (TEOS) doped with selenoxide or telluride are able to reduce the settlement of *Cypris* larvae of the barnacle *Balanus amphitrite* and larvae of the tubeworm *Hydroides elegans* in the presence of artificial seawater thanks to the formation of a thin layer of hypohalous acid at the coated surface.^[11] The photocatalytic reaction on the submarine surface is triggered by ultraviolet- and visible-light radiation, which easily penetrates sea water (reflection at moderate depths accounts to only 5–10%, while absorption is negligible).^[10] Selenide and telluride species, however, are derived from rare earth metals whereas the ZnO nanoparticles referred to above are toxic. Clearly, an AF/FR photocatalytic coating based on a nontoxic, readily available photocatalytic species would be highly desirable, as it would allow the main limitation on sol-gel-derived FR coatings to be overcome,^[12] that is, the limited antifouling activity.

We describe herein the first AF/FR photocatalytic coatings derived by the hydrolysis of TEOS and methyltriethoxysilane (MTES) in the presence of nanoflower-like Bi₂WO₆, followed by

[a] G. Scandura, Prof. G. Palmisano
Department of Chemical and Environmental Engineering
Institute Center for Water and Environment (iWater)
Masdar Institute of Science and Technology
PO BOX 54224, Abu Dhabi (United Arab Emirates)
E-mail: gpalmisano@masdar.ac.ae

[b] Dr. R. Ciriminna, Dr. M. Pagliaro
Istituto per lo Studio dei Materiali Nanostrutturati, CNR
via U. La Malfa 153, 90146 Palermo (Italy)
E-mail: mario.pagliaro@cnr.it

[c] Prof. Y.-J. Xu
State Key Laboratory of Photocatalysis on Energy and Environment
College of Chemistry and Chemical Engineering
Fuzhou University, Fuzhou 350002 (P. R. China)

Supporting information for this article is available on the WWW under <http://dx.doi.org/10.1002/chem.201600831>.

deposition on borosilicate glass slides (via spin-coating), condensation, and annealing at room temperature for one day (see the Supporting Information for the experimental details).

Nanostructured Bi_2WO_6 due to its narrow band gap (around 2.8 eV) is a low-cost, atoxic, highly efficient visible-light photocatalyst capable of absorbing visible light (which represents the majority of the solar irradiation) and to induce oxidation of numerous organic species.^[13] For instance, it is effective for the photocatalytic inactivation of *E. coli* and to eliminate marine microalgae as *Amphidium carterae* and *Tetraselmis suecica*.^[14] Thus, Bi_2WO_6 is a proper alternative to titanium dioxide (the most used photocatalyst active under UV irradiation). The possibility to prepare it in different nanostructured shapes, which allows better (photo)adsorption and electron-hole separation and hence a higher photoactivity, is another key advantage of this semiconductor, which is extremely active under visible light.

The films were prepared by using different amounts of MTES and Bi_2WO_6 in the sol. The nomenclature of the samples is the following: xxME-yyBW, where xx refers to the sol composition in terms of the mol% of Si-containing precursors, and yy refers to the concentration (in mM) of Bi_2WO_6 in the sol. Thus, a sol containing 10 mol% MTES and 90 mol% TEOS and no Bi_2WO_6 is indicated as 10ME-0BW. UV/Vis diffuse reflectance spectra show that the films with a higher degree of alkylation, entrapping the same amount of semiconductor, show larger absorption (Figure 1). As expected, absorption is higher for films con-

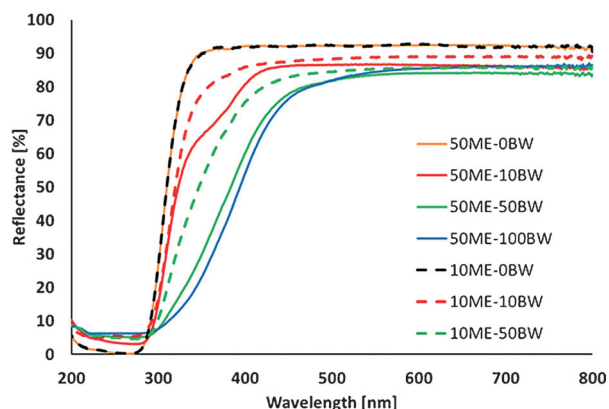


Figure 1. Diffuse reflectance spectra of films obtained at different percentages of MTES and at different loadings of Bi_2WO_6 .

taining increasing amounts of Bi_2WO_6 . The characterization and photocatalytic activity described in the following focus on films showing the highest absorption of visible radiation, namely, those derived from a sol-gel precursor mixture with TEOS/MTES = 1:1 molar ratio.

The SEM pictures show that all the prepared films share good microscopic uniformity (see the Supporting Information). Magnification of the 50ME-50BW film, for instance, renders clearly visible the Bi_2WO_6 nanoflowers encapsulated in the ORMOSIL film (Figure 2). The dimension of the semiconductor assemblies was found to be in the 2–5 μm range. Remarkably, the said dimension was not found to be influenced by the rela-

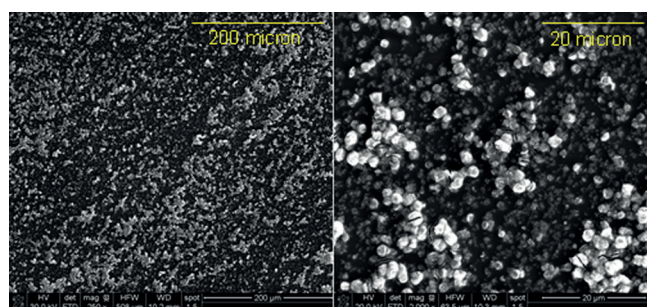


Figure 2. SEM images of a sample containing 50% MTES and a Bi_2WO_6 sol concentration of 50 mM (50ME-50BW).

tive amounts of both MTES and Bi_2WO_6 . Additionally, minor crackings are present in some particles, likely due to the higher surface tension on the flower-like semiconductor nanoparticles compared to the flat bare ORMOSIL film.

Cross-sectional image of the sample 50ME-50BW (Figure 3), obtained with SEM-FIB detectors, shows that the particles of Bi_2WO_6 are homogeneously encapsulated within the film, with

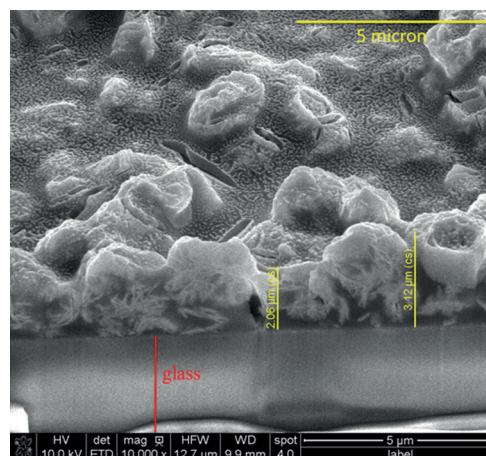


Figure 3. Cross-sectional image (by SEM-FIB) of the sample 50ME-50BW. The two vertical yellow bars are 2.06 and 3.12 μm . The red bar indicates the glass slide.

the semiconductor microparticles touching directly the glass substrate. Thus, the particles on one hand retain their flower-like structure, and on the other appear perfectly encapsulated by the ORMOSIL matrix. In fact, no leaching has been observed during the photocatalytic runs in water. Moreover the thickness measured in the cross-sectional image matches the values obtained by the profilometer (Figure 3). The distribution of Bi_2WO_6 on the film surface was further investigated by EDX mapping coupled to SEM imaging (Figure 4) allowing for detection of Si, Bi, and W and quantification of their ratios (see the Supporting Information for details). Focusing on an area with a high density of Bi_2WO_6 , the atomic ratios were Si/Bi/W = 81.6:12.2:6.2. As expected from stoichiometry, Bi/W is close to 2, which indicates a similar concentration of semiconductor particles in the sol, in the bulk of the film, and at the outer surface.

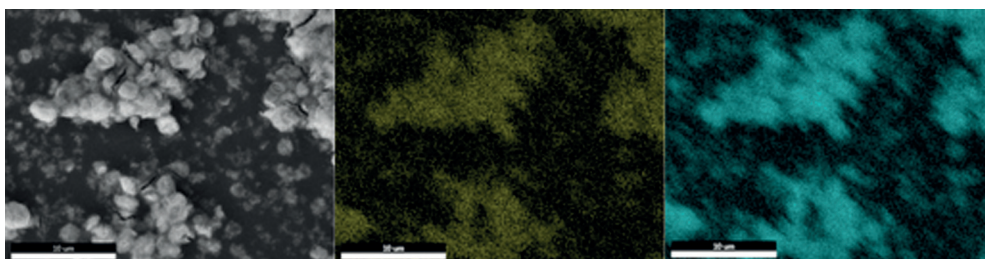


Figure 4. EDAX mapping of the SEM image reported on the left (sample 50ME-50BW). Yellow identifies W (centre) and blue identifies Bi (right). The bar is 10 μm .

A sample obtained through scratching the 50ME-100BW film with a stainless-steel spatula was examined by transmission electron microscopy. The resulting TEM image (Figure 5)

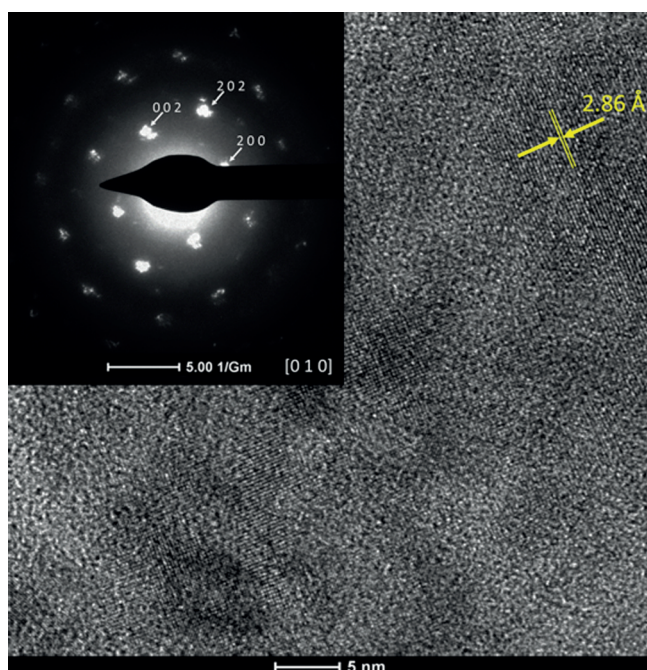


Figure 5. TEM image (scale bar, 5 nm) and, in the inset, SAED pattern (scale bar, 5 nm^{-1}) of the sample 50ME-50BW. Note that the spots in the SAED pattern are not sharp because of the presence of organosilica, which is amorphous, in the sample.

shows the presence of crystalline phases. The interplanar d -spacing (see the Supporting Information for details on calculations) was in the range 2.779–2.978 \AA . These values can be attributable to planes (131), (060), (002), and (200).^[15] The EDX spectrum (see the Supporting Information) and the SAED pattern (Figure 5) of this sample have confirmed that the observed crystalline regions correspond to the zone axis [010] of the orthorhombic structure of Bi_2WO_6 . The spot corresponding to the planes (002), (202), and (200) can be observed as indicated in the SAED figure.

Atomic force microscopy (AFM) investigation (Figure 6) confirms the smooth surface profile of the film on the nanoscale, with a RMS (root-mean-

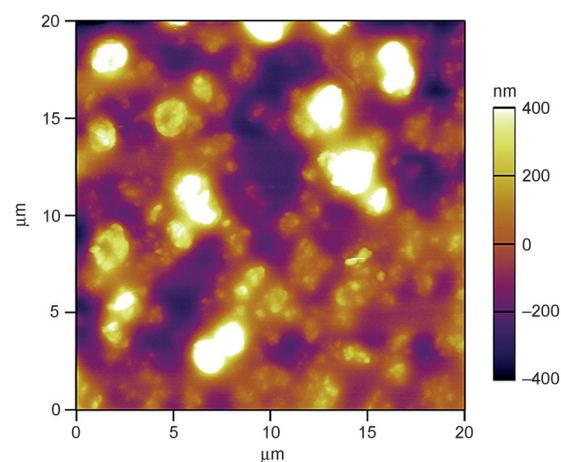


Figure 6. AFM image of a sample 50ME-50BW.

squared) roughness of 190 nm on a surface of 400 μm^2 . The white areas corresponding to the catalyst particles are in agreement with the previously highlighted dimensions unveiled by SEM-FIB analysis. Table 1 shows that the thickness of the film is 3.0–3.1 μm and it depends almost exclusively on the spin-coating parameters, rather than on the loading of Bi_2WO_6 or the MTES percentage.

The water contact angle (WCA) measurements in dark conditions denote a moderate hydrophilicity of all the samples. The said hydrophilicity, however, strongly increases upon irradiation with visible light, likely due to the formation of hydrogen bonds upon light activation of the photocatalyst in contact with water. Evidence of that is provided by the marked enhancement of the WCA decrease rate from 0.9 to 1.4 min^{-1} following increased Bi_2WO_6 loading from 10 to 100 mm (the WCA decrease is nearly linear, as shown in the Supporting Informa-

Table 1. Thickness, water contact angle (WCA), and adhesion energy of the solid and liquid surface (ΔW_{SLG}) of the films.

Sample	Thickness [μm]	WCA [$^\circ$] ^[a]	WCA decrease rate [$^\circ \text{min}^{-1}$] ^[b]	ΔW_{SLG} [mNm^{-1}]
50ME-10BW	3.1	67	0.90	100
50ME-50BW	3.0	74	1.2	91.8
50ME-100BW	3.0	64	1.4	103

[a] In the dark. [b] Under visible radiation.

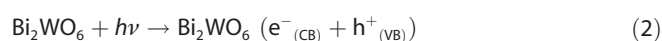
tion). The adhesion energy per unit area of the solid and liquid surface (ΔW_{SLG}) was estimated by means of the Young–Dupré equation, in which γ_{LG} is the water–air surface tension, equal to approximately 72 mNm^{-1} at room temperature, and θ is the experimental contact angle:^[16]

$$\Delta W_{\text{SLG}} = \gamma_{\text{LG}}(1 + \cos \theta) \quad (1)$$

The activity of the prepared films, deposited on glass, was initially tested in static demineralized water, under visible-light irradiation ($\lambda > 400 \text{ nm}$) by a 100 W halogen lamp with a UV cut-off filter. To our delight, after 90 min hydrogen peroxide was found to be present in solution with a concentration increasing with the loading of Bi_2WO_6 (Table 2). H_2O_2 is a strong

Table 2. H_2O_2 production from an ORMOSIL film doped with Bi_2WO_6 after 90 min of visible-light irradiation.	
Sample	H_2O_2 concentration [μM]
50ME–10BW	5.29 ± 0.59
50ME–50BW	6.76 ± 1.17
50ME–100BW	10.3 ± 1.8

and clean oxidant, able to rapidly degrade the (bio)organic species adsorbed onto the film making the surface inhospitable to the settling larvae of fouling organisms, thanks to fast decomposition into water and oxygen by a free-radical intermediate that prevents the attachment of hard foulants.^[17] At the film–water interface, the following reaction mechanism can be postulated:^[18] the particles encapsulated on the film absorb the visible radiation generating electron–hole pairs. The electrons then combine with molecular oxygen giving rise to a series of radical species that are very reactive and able to eventually yield H_2O_2 . The mechanism can be schematized as follows:



Equations like those in (2–6) are also presented when TiO_2 is used in photocatalysis (see for instance ref. [18]) but under visible light (without UV irradiation) the reaction rates with titania are very low, and in addition the electron–hole pair recombination rate plays a more relevant role. Results in Table 2 demonstrate how the production of H_2O_2 can be dramatically increased by using Bi_2WO_6 in the nano-flower-like structure, further encapsulated in the ORMOSIL thin film, similarly to what happens with encapsulation in plain silica.^[20]

No leaching of Bi_2WO_6 was observed into the supernatant solution, even after three months immersion, and after repeated irradiation cycles. It is also worth noting that, when the film is applied on a surface constantly exposed to solar radiation, the continuous production of H_2O_2 will inhibit the formation of (bio)fouling matter on the protected material. The antifouling performance of the coating was tested using uracil as a model biomolecule. The film 50ME–100BW immersed in aqueous solution of uracil (1 ppm) was irradiated by simulated solar light (see the Supporting Information for details). Under these conditions, the photocatalytic degradation of the uracil is roughly linear with time and the conversion was about 40% after three days (Figure 7).

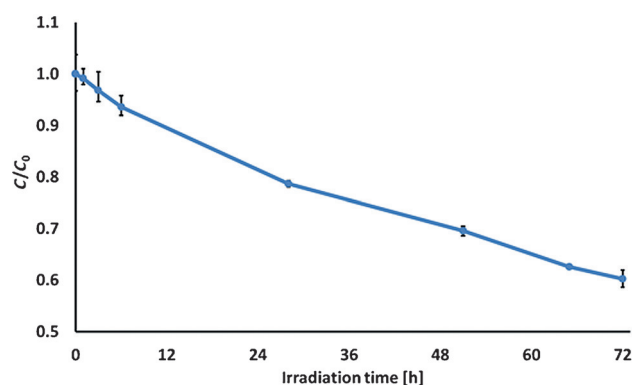


Figure 7. Photocatalytic disappearance of uracil versus irradiation time. The curve is the average of three runs. $C_0 = 1 \text{ ppm}$, initial concentration of uracil.

To investigate the foul release properties of the films, adsorption of adenine (6-aminopurine), an hydrophilic biomolecule, was also studied. First, 1 mL of 1 gL^{-1} adenine aqueous solution was dropped on the 50ME–100BW sample film. The coating was kept at 40°C for 12 h to allow solvent evaporation. The FTIR spectrum of the film treated with adenine clearly shows several new bands relative to adsorbed adenine (Figure 8). The same film was immersed in water for 2 h, and the FTIR analysis was repeated after withdrawing the coating.

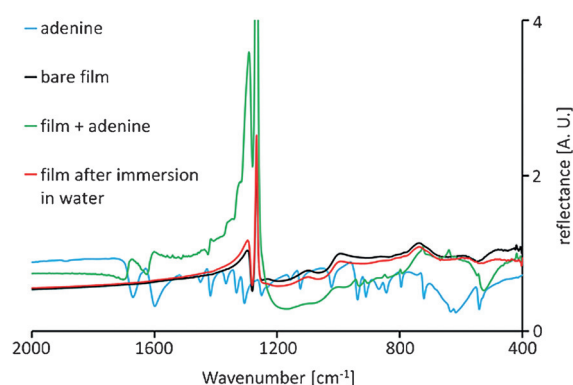


Figure 8. FTIR spectra of the 50ME–100BW sample: bare film (black curve), film with adsorbed adenine (green curve), and film after 2 h immersion in water (red curve). The light blue curve refers to the pure adenine. See the Supporting Information for the complete spectra.

Remarkably, all adenine peaks disappeared (Figure 8) showing that the limited hydrophilicity of the film produces the fast release of the previously adsorbed adenine, even in the absence of direct light irradiation. Adenine derivative adenosine bonded with one to three phosphoric acid units yields AMP, ADP, and ATP, which have a variety of roles in biochemistry.

In conclusion, we have developed the first series of ORMOSIL-based AF/FR coatings (*AquaSun*) based on the encapsulation of the readily available, nontoxic bismuth wolframate in nanostructured, flower-like morphology. The coatings are leach-proof and conjugate the ORMOSIL excellent HLB which gives place to foul-releasing properties, with improved anti-fouling action due to H₂O₂ formed at the coating–water interface.

It is anticipated that the new coating might have plenty of applications to prevent biofouling of intake structures, systems piping seawater and heat-exchanger tubes (in desalination and power plants). Commercially available ORMOSIL-based FR formulations (*AquaFast*)^[19] will shortly be complemented with 2nd generation AF/FR xerogel coatings providing immersed surfaces, including vessels of different size and composition, with enhanced ecofriendly protection from biofouling.

Acknowledgements

This work is dedicated to the University at Buffalo's Profs. M.R. Detty and F.V. Bright for their exceptional work on xerogel foul-release coatings. We thank Dr. Francesco Genoese, Fincantieri and Distretto Silicia Navtec, for valued assistance during the STI-TAM project. Thanks to Thomas Delclos, Cyril Aubry, and Chia-Yun Lai for their assistance with FT-IR, SEM-EDX, and AFM measurements, respectively. Masdar Institute of Science and Technology (Abu Dhabi) and MIUR (Rome) is gratefully acknowledged for funding part of this work (project FA2014-000010, Masdar) and (PON02_00153_2849085, MIUR).

Keywords: antifouling · AquaSun · hydrogen peroxide · photocatalytic · xerogel

- [1] a) M. P. Schultz, *Biofouling* **2007**, *23*, 331; b) R. L. Townsin, *Biofouling* **2003**, *19*, 9.
- [2] M. P. Schultz, J. A. Bendick, E. R. Holm, W. M. Hertel, *Biofouling* **2010**, *27*, 87.
- [3] R. Kattan, *Cleaning up Marine Antifouling*, *IMarEST*, London, 29 April **2010**.
- [4] D. Williams, *Challenges in developing antifouling coatings*, *IMarEST*, London, 29 April **2010**.
- [5] a) R. Ciriminna, F. V. Bright, M. Pagliaro, *ACS Sustainable Chem. Eng.* **2015**, *3*, 559; b) J. E. Gittens, T. J. Smith, R. Suleiman, R. Akid, *Biotechnol. Adv.* **2013**, *31*, 1738.
- [6] R. S. Morris, M. A. Walsh, U.S. Patent US 5916947A.
- [7] M. Pagliaro, R. Ciriminna, G. Palmisano, *J. Mater. Chem.* **2009**, *19*, 3116.
- [8] a) C. J. Brinker and G. W. Scherer, *Sol-gel science: the physics and chemistry of sol-gel processing*, **1990**, Academic Press: New York; b) D. Avnir, *Acc. Chem. Res.* **1995**, *28*, 328; c) B. C. Dave, H. Soyez, M. J. Miller, B. Dunn, J. S. Valentine, J. I. Zink, *Chem. Mater.* **1995**, *7*, 1431.
- [9] a) S. Pandey, G. A. Baker, M. A. Kane, N. J. Bonzagni, F. V. Bright, *Chem. Mater.* **2000**, *12*, 3547; b) Y. Tang, E. C. Tehan, Z. Y. Tao, F. V. Bright, *Anal. Chem.* **2003**, *75*, 2407.
- [10] D. M. McMaster, S. M. Bennett, Y. Tang, J. A. Finlay, G. L. Kowalke, B. Nedved, F. V. Bright, M. E. Callow, J. A. Callow, D. E. Wendt, M. G. Hadfield, M. R. Detty, *Biofouling* **2009**, *25*, 21.
- [11] Z. Lee, C. Hu, S. Shang, K. Du, M. Lewis, R. Arnone, R. Brewin, *J. Geophys. Res. [Oceans]* **2013**, *118*, 4241.
- [12] M. R. Detty, R. Ciriminna, F. V. Bright, M. Pagliaro, *Acc. Chem. Res.* **2014**, *47*, 678.
- [13] N. Zhang, R. Ciriminna, M. Pagliaro, Y. J. Xu, *Chem. Soc. Rev.* **2014**, *43*, 5276.
- [14] a) J. Ren, W. Wang, L. Zhang, J. Chang, S. Hu, *Catal. Commun.* **2009**, *10*, 1940; b) S. Obregón Alfaro, A. Martínez-de la Cruz, L. M. Torres-Martínez, S. W. Lee, *Catal. Commun.* **2010**, *11*, 326.
- [15] K. S. Knight, *Mineralogical Magazine* **1992**, *56*, 399.
- [16] J. N. Israelachvili, *Intermolecular and Surface Forces*, Academic Press: London, 1992.
- [17] S. Møller Olsen, J. B. Kristensen, B. S. Laursen, L. T. Pedersen, K. Dam-Johansen, S. Kiil, *Prog. Org. Coat.* **2010**, *68*, 248.
- [18] M. R. Hoffmann, S. T. Martin, W. Choi, D. W. Bahnemann, *Chem. Rev.* **1995**, *95*, 69.
- [19] M. R. Detty, R. Ciriminna, F. V. Bright, M. Pagliaro, *ChemNanoMat.* **2015**, *1*, 148.
- [20] Y. Zhang, R. Ciriminna, G. Palmisano, Y.-J. Xu, M. Pagliaro, *RSC Adv.* **2014**, *4*, 18341–18346.

Received: February 22, 2016

Published online on April 18, 2016